

See discussions, stats, and author profiles for this publication at: <https://www.researchgate.net/publication/262146043>

# Major Change in Regiospecificity for the Exo-1,3- $\beta$ -glucanase from *Candida albicans* following Its Conversion to a Glycosynthase

ARTICLE *in* BIOCHEMISTRY · MAY 2014

Impact Factor: 3.02 · DOI: 10.1021/bi500239m · Source: PubMed

---

READS

13

4 AUTHORS, INCLUDING:



**Yoshio Nakatani**

University of Otago

14 PUBLICATIONS 111 CITATIONS

SEE PROFILE

# Major Change in Regiospecificity for the Exo-1,3- $\beta$ -glucanase from *Candida albicans* following Its Conversion to a Glycosynthase

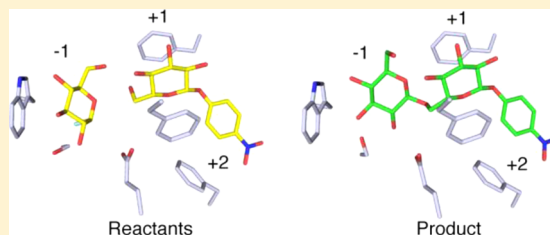
Y. Nakatani,<sup>†</sup> D. S. Larsen,<sup>‡</sup> S. M. Cutfield,<sup>†</sup> and J. F. Cutfield<sup>\*,†</sup>

<sup>†</sup>Biochemistry Department, University of Otago, P.O. Box 56, Dunedin 9054, New Zealand

<sup>‡</sup>Chemistry Department, University of Otago, P.O. Box 56, Dunedin 9054, New Zealand

## S Supporting Information

**ABSTRACT:** The exo-1,3- $\beta$ -glucanase (Exg) from *Candida albicans* is involved in cell wall  $\beta$ -D-glucan metabolism and morphogenesis through its hydrolase and transglycosidase activities. Previous work has shown that both these activities strongly favor  $\beta$ -1,3-linkages. The E292S Exg variant displayed modest glycosynthase activity using  $\alpha$ -D-glucopyranosyl fluoride ( $\alpha$ -GlcF) as the donor and pNP- $\beta$ -D-glucopyranoside (pNPGlc) as the acceptor but surprisingly showed a marked preference for synthesizing  $\beta$ -1,6-linked over  $\beta$ -1,3- and  $\beta$ -1,4-linked disaccharide products. With pNPXyl as the acceptor, the preference became  $\beta$ -1,4 over  $\beta$ -1,3. The crystal structure of the glycosynthase bound to both of its substrates,  $\alpha$ -GlcF and pNPGlc, is the first such ternary complex structure to be determined. The results revealed that the donor bound in the  $-1$  subsite, as expected, while the acceptor was oriented in the  $+1$  subsite to facilitate  $\beta$ -1,6-linkage, thereby supporting the results from solution studies. A second crystal structure containing the major product of glycosynthesis, pNP-gentiobiose, showed that the  $-1$  subsite allows another docking position for the terminal sugar; i.e., one position is set up for catalysis, whereas the other is an intermediate stage prior to the displacement of water from the active site by the incoming sugar hydroxyls. The  $+1$  subsite, an aromatic “clamp”, permits several different sugar positions and orientations, including a  $180^\circ$  flip that explains the observed variable regiospecificity. The *p*-nitrophenyl group on the acceptor most likely influences the unexpectedly observed  $\beta$ -1,6-specificity through its interaction with F229. These results demonstrate that tailoring the specificity of a particular glycosynthase depends not only on the chemical structure of the acceptor but also on understanding the structural basis of the promiscuity of the native enzyme.



A major advance in carbohydrate synthesis, specifically the ability to form new glycosidic linkages, was realized when engineered mutations directed at the catalytic nucleophile (carboxylate group) of a retaining  $\beta$ -glycosidase, in conjunction with the use of a mimic of the glycosyl enzyme intermediate [ $\alpha$ -D-glucopyranosyl fluoride (Figure 1, compound 1)] as the donor, allowed the enzyme to act as a “glycosynthase” and add a glucosyl residue to an acceptor alcohol to form a new oligosaccharide species.<sup>1,2</sup> Successful substitutions include serine, alanine, and glycine, which prevent enzymatic hydrolysis of the accumulating product. The advantages that such modified enzymes offer with regard to stereo- and regiospecificity make them attractive alternatives to existing chemical methods. Since that time, many such glycosynthases have been made and some further refined by directed evolution, and in conjunction with an increasing variety of donors and especially acceptors, an ever-expanding collection of novel carbohydrate compounds has resulted.<sup>3–8</sup>

While the formation of mixed products containing different linkages has been widely reported for individual glycosynthases under various conditions, in general the regiospecificity displayed by a particular glycosynthase is the same as the regiospecificity that the wild type enzyme shows for its hydrolysis and/or transglycosylation reactions. This is particularly true for endoglycosidases whereas exoglycosidases display

more variation.<sup>9</sup> Interactions of the acceptor species, often an aryl glycoside, at the  $+1$  and  $+2$  sugar-binding subsites on the enzyme were deduced to be important determinants of regiospecificity for the glycosynthase derivatives of  $\beta$ -glucosidases from *Streptomyces* sp. and *Agrobacterium* sp.<sup>10,11</sup> Thus, depending on the structure of the acceptor, different orientations may be possible for the presentation of a particular hydroxyl group for glycosylation. Most of the exoglycosidase-related glycosynthases described in the literature have been glycosynthases derived from the CAZy<sup>12</sup> GH1 family  $\beta$ -glucosidases (EC 3.2.1.21).

Glucan exo-1,3- $\beta$ -glucosidases (EC 3.2.1.58) are found within families GH3, -5, -17, and -55. The exo-1,3- $\beta$ -glucanase (Exg) from *Candida albicans*, a retaining glycosidase in the GH5 family, is secreted into the cell wall where it is believed to participate in cell wall glucan metabolism and morphogenesis because of its hydrolase and transglycosidase activities at the nonreducing ends of glucan polymers.<sup>13,14</sup> In *C. albicans*,  $\beta$ -D-glucans are the major structural components of the cell wall, present as branched polymers of  $\beta$ -1,3- and  $\beta$ -1,6-glucan.<sup>15,16</sup> Stubbs et al.<sup>17</sup> established that, as a hydrolase, Exg shows an at

Received: February 24, 2014

Revised: May 6, 2014

Published: May 7, 2014



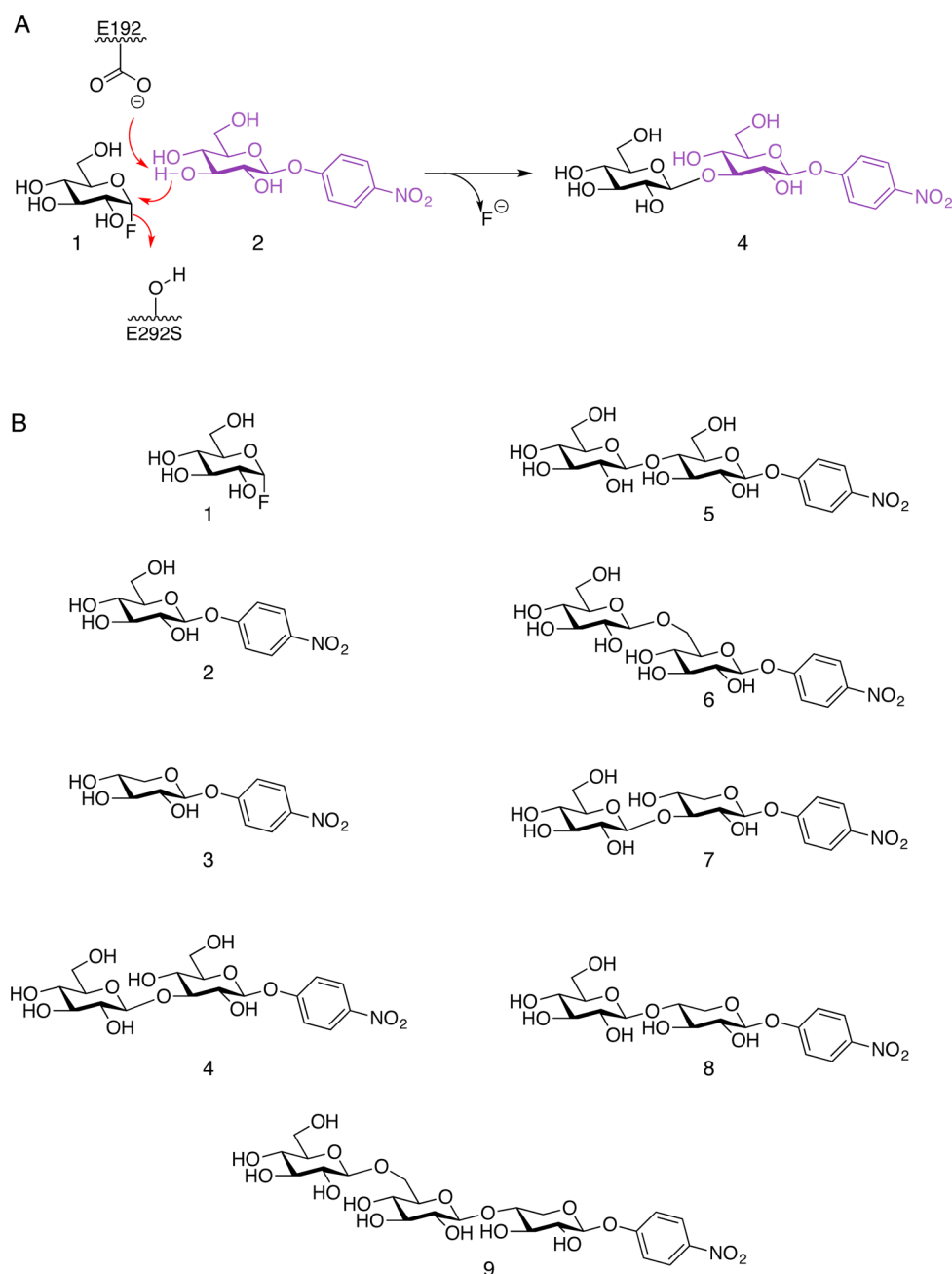


**Figure 1.** (A) Mechanism and expected regiospecificity for the glycosynthase reaction involving the E292S exo-1,3-β-glucanase variant from *C. albicans* (figure adapted from ref 1). (B) Structures of donor (1), acceptor (2 and 3), and product (4–9) species relevant to this study.

least 1000-fold preference for β-1,3-glycosidic linkages over β-1,6- and β-1,4-linkages. Similarly, their analysis of the transglucosylation activity showed only the presence of β-1,3-linkages in the linear oligosaccharide products isolated. It was concluded that Exg was a very efficient transglucosidase, given yields of 40–50% achieved using substrate concentrations of 2–8% (w/v). Around the same time, we determined the crystal structure of Exg in native and inhibitor-bound forms<sup>18</sup> but were not able to directly confirm the specificity for β-1,3-linkages from these studies. More recently, we investigated the role of a phenylalanine clamp at the +1 sugar-binding subsite<sup>19</sup> and established its importance in directing the binding of the substrate through CH–π interactions. A likely +2 subsite was also identified. The interactions at these sites were thought to be responsible for the β-1,3-specificity shown by the enzyme.

Preliminary studies using Exg in which the catalytic nucleophile Glu 292 was mutated to serine showed that this variant acted as a sluggish glycosynthase, thereby providing the possibility of studying a “productive” complex in crystal. Here we describe the crystallographic analysis of the E292S Exg glycosynthase in complex with donor and acceptor molecules as well as with the major disaccharide product. Coupled with solution studies that showed that additional products were formed, this work has revealed a significant change in regiospecificity preference between wild-type Exg and its glycosynthase variant. It also provides major insights into how the enzyme is able to organize variable sugar binding at the –1, +1, and +2 subsites.

## EXPERIMENTAL PROCEDURES

**Materials.**  $\alpha$ -D-Glucopyranosyl fluoride ( $\alpha$ -GlcF) was provided by S. G. Withers (University of British Columbia, Vancouver, BC); *p*-nitrophenyl  $\beta$ -D-gentiobiose was synthesized in house. All other reagents, including the acceptors *p*-nitrophenyl  $\beta$ -D-glucopyranoside (pNPGlc) and *p*-nitrophenyl  $\beta$ -D-xylopyranoside (pNPXyl), were purchased from Sigma-Aldrich (Oakville, ON).

**Exg Glycosynthase Preparation.** Exg variants E292S and E292G were made and subsequently tested for glycosynthase activity. The following oligonucleotides were used to generate mutations at E292: 5'-GG AAC GTC GCT GGT TCA TGG TCT GCT GCT TTG-3' (forward) and 5'-CAA AGC AGC AGA CCA TGA ACC AGC GAC GTT CC-3' (reverse) for E292S and 5'-GTC GCT GGT GGA TGG TCT GCT-3' (forward) and 5'-AGC AGA CCA TCC ACC AGC GAC-3' (reverse) for E292G (positions of mismatches underlined). Mutations were introduced using recombinant polymerase chain reaction,<sup>20</sup> and the constructs were DNA-sequenced to confirm the mutations. The modified genes were expressed in *Pichia pastoris* strain KM71 (Invitrogen) and the secreted recombinant proteins purified by hydrophobic interaction chromatography using Phenyl Superose HR 5/5 columns (Pharmacia LKB Biotechnology AB), with all methods essentially as previously described.<sup>19</sup> Both variants were tested for residual hydrolysis activity using laminarin (a  $\beta$ -1,3-glucan) as the substrate.<sup>17</sup>

**Glycosynthesis Reactions.** Glycosynthesis reactions were conducted using 20 mM  $\alpha$ -D-glucopyranosyl fluoride [ $\alpha$ -GlcF (compound 1 in Figure 1)] as the donor, 15 mM *p*-nitrophenyl  $\beta$ -D-glucopyranoside [pNPGlc (compound 2 in Figure 1)], or 15 mM *p*-nitrophenyl  $\beta$ -D-xylopyranoside [pNPXyl (compound 3 in Figure 1)] as the acceptor and 0.25 mg mL<sup>-1</sup> E292S Exg in 50 mM sodium phosphate buffer (pH 6.0) at 30 °C. The rate of glycosynthesis was initially monitored using thin layer chromatography in which samples were spotted onto a silica gel 60 F<sub>254</sub> plate with an acetic acid/methanol/water [7:2:1 (v/v)] solvent system. The *p*-nitrophenyl (pNP) derivatives were detected under UV light, soaked in 10% sulfuric acid, and heated at 160 °C (for 5–10 min) to detect oligosaccharides.

For time course experiments, the reaction volume was 600  $\mu$ L. HPLC analysis was conducted using a  $\mu$ Bondapak C18 column (Waters Associates) coupled to a Gilson HPLC system (model 321 pump, model UV/vis-156 detector, and model 215 liquid handler). The column was equilibrated with 6% (v/v) aqueous methanol before a 50  $\mu$ L sample was loaded. Isocratic elution was performed at a flow rate of 1.0 mL min<sup>-1</sup>. The pNP derivatives were detected at 300 nm. The dual UV detector was also set to 405 nm to detect *p*-nitrophenol. Individual peaks were collected and analyzed by TLC for comparison. The reaction was monitored over 120 h, and amounts of products formed were estimated by peak integration.

A larger scale separation of products, to allow full chemical characterization, was conducted following a 48 h incubation of a 5 mL reaction mixture. Samples (500  $\mu$ L) were loaded onto a LichroCART C18 column (Merck) and eluted at a rate of 2 mL min<sup>-1</sup>, in the following sequence: 100% water, 0 to 20% (v/v) methanol gradient over 5 min, 20 min isocratic flow, 20 to 40% (v/v) methanol gradient over 40 min, 5 min isocratic flow, and finally 40 to 100% (v/v) methanol for 10 min. Equivalent peak fractions were combined, freeze-dried, and then analyzed by NMR and mass spectrometry.

**NMR Spectroscopy.** <sup>1</sup>H and <sup>13</sup>C NMR spectra of solutions in D<sub>2</sub>O were recorded at 25 °C, externally referenced to sodium 3-(trimethylsilyl)propionate at 500 and 125 MHz, respectively, on a Varian Unity INOVA 500 MHz spectrometer (Department of Chemistry, University of Otago) using standard pulse sequences.

**Mass Spectrometry.** HPLC fractions were analyzed by electrospray ionization (ESI)-coupled mass spectrometry using an LCQ Deca ion trap mass spectrometer (Thermo Scientific, San Jose, CA). Concentrated fractions were directly injected into the ESI source using a syringe pump. Mass spectra were acquired in positive ion mode over a mass range of *m/z* 200–2000.

**Crystallography.** Crystals of E292S Exg were obtained using the microbatch method. Drops containing 1  $\mu$ L of protein (5–20 mg mL<sup>-1</sup>) and 1  $\mu$ L of a precipitant solution [200 mM CaCl<sub>2</sub>, 100 mM HEPES-KOH (pH 7.3), and 19–24% (w/v) PEG 8000] were layered under 100  $\mu$ L of paraffin oil and incubated at 18 °C.

For complex formation, an E292S Exg crystal was soaked in 10  $\mu$ L of mother liquor containing 15 mM  $\alpha$ -GlcF and left for 20 min before the addition of ~60  $\mu$ g of solid pNPGlc. The soaked crystal was left for 7 h at room temperature, transferred to a solution of 10% (v/v) glycerol-containing mother liquor, and flash-frozen. For the complex with pNP-gentiobiose, 1 mg of compound was dissolved in 20  $\mu$ L of mother liquor, and crystals were soaked for 3 h at room temperature, dipped into cryo-protectant oil, and flash-frozen.

Diffraction data for E292S Exg and the ternary complex were collected at room temperature (capillary mounted) and 113 K, respectively, on a Rigaku RU-300/MAR 345 image plate system at the University of Auckland Structural Biology Laboratory (Auckland, New Zealand), whereas data for the binary complex were collected from a Rigaku R-Axis IV++ image plate system at 113 K at the University of Otago Biochemistry Department.

Data were processed using the CCP4 program suite<sup>21</sup> and the structures determined by molecular replacement using PHASER.<sup>22</sup> Coot<sup>23</sup> was used for model building, and structures were refined using PHENIX<sup>24</sup> with validation by SFCHECK.<sup>25</sup> Ligand structures were built into Omit difference maps. Structures were drawn using PyMOL Molecular Graphics System version 1.5.0.4 (Schrödinger, LLC, Portland, OR). Protein–ligand interactions are presented as LIGPLOT diagrams.<sup>26</sup>

## RESULTS

Site-directed mutagenesis of the catalytic nucleophile E292 codon followed by overexpression in *P. pastoris*, produced E292S and E292G variants that were purified to homogeneity using hydrophobic interaction chromatography, essentially as described previously for the WT and other mutants.<sup>19</sup> Glycosynthase activity was assessed using  $\alpha$ -GlcF as the donor and pNPGlc as the acceptor (Figure 1). TLC analysis showed that both variants were active but that product formation was slow (measured over 24–48 h). It was also found that the E292G variant showed a small amount of hydrolytic activity (<0.01% of that of the WT) toward  $\beta$ -1,3-linked substrates (Figure S1A of the Supporting Information); thus, E292S Exg was employed exclusively for further studies.

**Glycosynthesis Reaction Products.** The glycosynthesis reaction was initially studied using pNPGlc as the acceptor. A preliminary experiment showed slow product formation as analyzed using TLC (Figure 2A). Three main pNP-derivatized



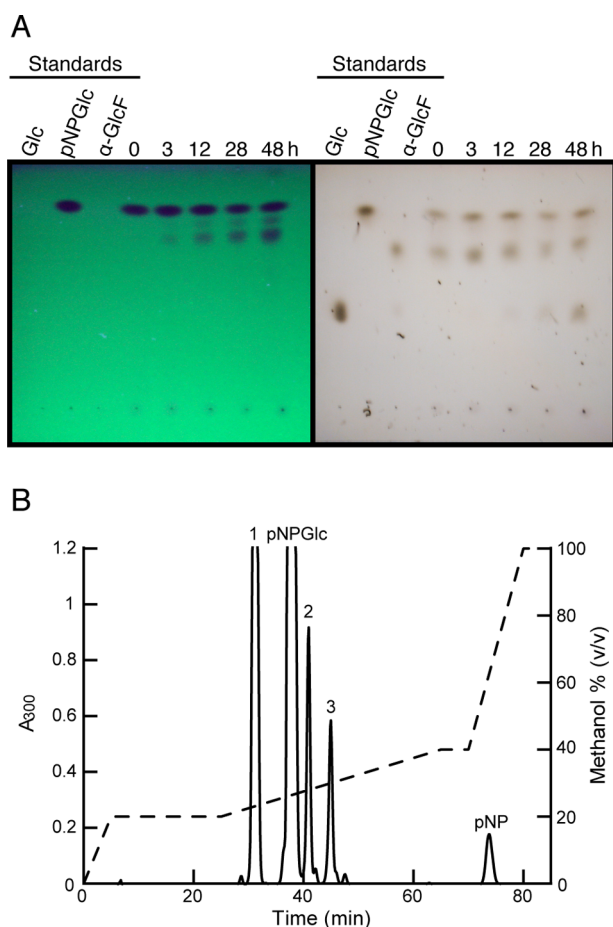


**Figure 2.** Separation of glycosynthesis products following a 48 h incubation of the reaction mixture containing  $\alpha$ -GlcF as the donor and pNPGlc as the acceptor, in the presence of E292S Exg (see Experimental Procedures). (A) TLC analysis showing accumulation over time of one major and one minor species (shown to be a mixture). Detection under UV light shows pNP derivatives (left); sulfuric acid–heat treatment shows carbohydrate compounds present. (B) RP-HPLC profile showing elution of pNP derivatives in aqueous methanol, detected at 300 nm. The peaks at 30, 42, and 45 min were subsequently identified as pNP-gentiobioside (compound 6), pNP-laminaribioside (compound 4), and pNP-cellobioside (compound 5), respectively.

product fractions could clearly be distinguished using HPLC (Figure 2B and Figure S1B of the Supporting Information), and these were all shown to contain disaccharide structures. NMR data are given in full in the Supporting Information.

The mass spectrum of the major fraction exhibited peaks at  $m/z$  486.3 and 949.0 that were attributed to composite ions  $MNa^+$  and  $M_2Na^+$ , respectively, consistent with the structure of the *p*-nitrophenyl glycoside of a disaccharide containing two glucose residues. The  $^{13}C$  NMR spectrum supported this interpretation; moreover, the observed downfield shift of the resonance for C6 relative to C6' indicated a 1  $\rightarrow$  6 linkage. The structure of this compound was identified unambiguously on the basis of strong three-bond correlations between H6 and C1', and between C6 and H1', evident in the gHMBC spectrum, and by a clear correlation between the inter-residue anomeric protons H1' and H6 in the NOESY spectrum. Assignment of a  $\beta$ -anomeric configuration for the new glycosidic linkage was based on the coupling constant  $^3J_{1,2'}$  for H1' ( $\delta$  4.70) of 7.9 Hz. These data are consistent with

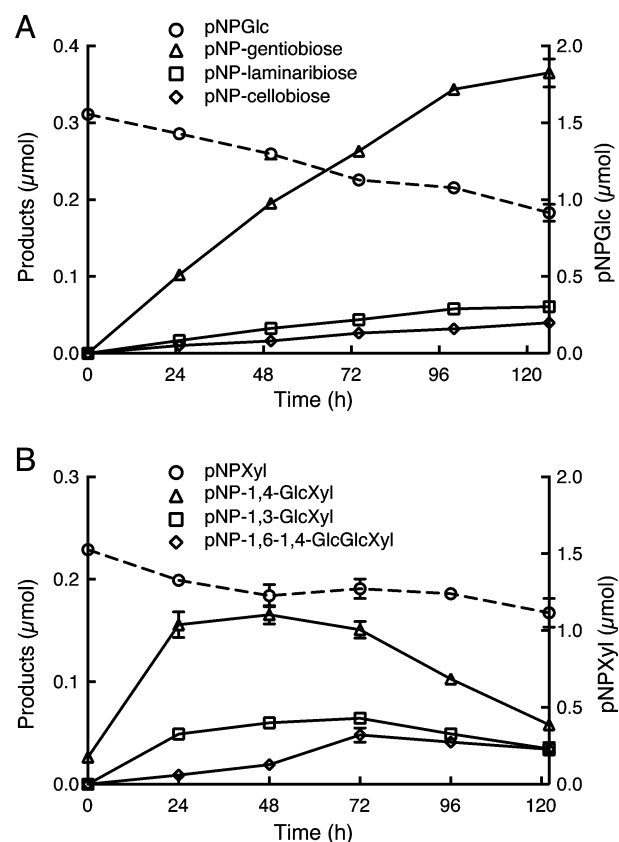


**Figure 3.** Time course of glycosynthesis reactions over 120 h, using  $\alpha$ -GlcF as the donor and pNPGlc (A) or pNPXyl (B) as the acceptor. Solid lines show accumulation of the three main products, and dashed lines show the decrease in the level of the acceptor.

NMR data reported previously.<sup>27,28</sup> Therefore, we can conclude that the major product of the glycosynthase reaction was *p*-nitrophenyl 6-*O*-( $\beta$ -D-glucopyranosyl)- $\beta$ -D-glucopyranoside [pNP-gentiobioside (Figure 1, compound 6)].

The second HPLC fraction consisted mainly of a pNP-disaccharide product as seen from the NMR data but also contained a small amount of pNP-trisaccharide on the basis of its ESI mass spectrum. Because of the lack of material, the  $^{13}C$  NMR data could be obtained only indirectly from the cross-peaks in the HSQC spectrum. The downfield shift of the resonance for C3 relative to C3' is indicative of a 1  $\rightarrow$  3 linked disaccharide and was confirmed by a cross-peak between the signal for the interglycosidic anomeric proton, H1', and C3 in the HMBC spectrum. The  $^1H$  NMR spectrum shows the anomeric proton H1' resonates as a doublet at  $\delta$  4.70 with a coupling constant  $^3J_{1,2}$  of 7.9 Hz, indicating a  $\beta$ -anomeric configuration of the glycosidic linkage. The data were consistent with those reported previously<sup>10,27,28</sup> for *p*-nitrophenyl 3-*O*-( $\beta$ -D-glucopyranosyl)- $\beta$ -D-glucopyranoside [pNP-laminaribioside (Figure 1, compound 4)].

Fraction 3 contained the least material and was found to be a mixture of disaccharide and trisaccharide from the MS data. Despite the low yield, a combination of  $^1H$  NMR,  $^{13}C$  NMR, HSQC, NOESY, and COSY spectra were of sufficient resolution to identify the pNP-disaccharide containing a  $\beta$  1  $\rightarrow$  4 linkage as the major component of the mixture. Thus, the third most abundant product of the glycosynthesis reaction is *p*-nitrophenyl 4-*O*-( $\beta$ -D-glucopyranosyl)- $\beta$ -D-glucopyranoside

**Table 1. X-ray Data Processing and Refinement Statistics**

	E292S Exg (apoenzyme)	with $\alpha$ -GlcF and pNPGlc (complex)	with pNP-gentiobiose (complex)
wavelength (Å)	1.54	1.54	1.54
resolution (outer shell) (Å)	26.2–1.85 (1.95–1.85)	37.0–1.86 (1.96–1.86)	39.4–1.59 (1.68–1.59)
space group	$P2_12_12_1$	$P2_12_12_1$	$P2_12_12_1$
unit cell parameters	$a = 60.0$ Å $b = 65.3$ Å $c = 96.9$ Å $\alpha = \beta = \gamma = 90^\circ$	$a = 59.0$ Å $b = 64.2$ Å $c = 95.0$ Å $\alpha = \beta = \gamma = 90^\circ$	$a = 58.8$ Å $b = 64.3$ Å $c = 94.5$ Å $\alpha = \beta = \gamma = 90^\circ$
$R_{\text{sym}}$ (outer shell)	0.080 (0.364)	0.088 (0.527)	0.027 (0.212)
mean $I/\sigma I$ (outer shell)	12.3 (4.0)	15.5 (2.7)	39.2 (6.9)
completeness (outer shell)	98.4 (89.2)	90.7 (74.0)	99.0 (93.7)
multiplicity (outer shell)	4.0 (3.9)	5.2 (3.9)	5.6 (4.7)
total no. of reflections	130835 (16400)	147555 (12881)	271932 (30855)
no. of unique reflections	32719 (4253)	28249 (3304)	48285 (6562)
$R_{\text{cryst}}$	0.14 (0.24)	0.15 (0.24)	0.15 (0.19)
$R_{\text{free}}$	0.18 (0.28)	0.21 (0.29)	0.18 (0.23)
rmsd for bonds (Å)	0.007	0.007	0.006
rmsd for angles (deg)	1.06	1.04	1.08
rmsd for chiral volume (Å <sup>3</sup> )	0.077	0.075	0.073
no. of protein atoms	3240	3229	3258
no. of ligand atoms	—	39 <sup>a</sup>	53 <sup>b</sup>
no. of water atoms	311	492	486
average main chain $B$ factor (Å <sup>2</sup> )	12.7	12.9	13.5
average side chain $B$ factor (Å <sup>2</sup> )	16.3	14.5	16.0
average ligand $B$ factor (Å <sup>2</sup> ) for $\alpha$ -GlcF	—	10.8	—
average ligand $B$ factor (Å <sup>2</sup> ) for pNPGlc	—	23.6	—
average ligand $B$ factor (Å <sup>2</sup> ) for pNP-gentiobiose	—	—	16.7
average water $B$ factor (Å <sup>2</sup> )	25.4	23.5	26.5
PDB entry	4M80	4M81	4M82

<sup>a</sup> $\alpha$ -GlcF, pNPGlc, and glycerol. <sup>b</sup>pNP-gentiobiose, glucose (secondary binding site), and ethylene glycol (2).

[pNP-cellobioside (Figure 1, compound 5)]. The NMR data were consistent with those recently reported by Wei et al.<sup>29</sup>

A time course study over 120 h showed that the three disaccharide products accumulated over this time with initial rates of formation in a 100:16:9 ratio (Figure 3A). It is clear from these results that  $\beta$ -1,6-linkage formation was strongly favored, a finding seemingly at odds with the known  $\beta$ -1,3-specificity of the wild-type enzyme.

A second experiment involved analysis of E292S Exg glycosynthase products using *p*-nitrophenyl  $\beta$ -D-xylopyranoside (pNPXyl) as the acceptor, thereby removing the possibility of forming  $\beta$ -1,6-linkages with the donor  $\alpha$ -GlcF. Three different reaction products were identified (see Figure S2 of the Supporting Information) and separated by RP-HPLC as described above. The time course of the reaction is shown in Figure 3B with products identified by mass spectrometry and <sup>1</sup>H and <sup>13</sup>C NMR analysis. Linkage types were confirmed by analysis of two-dimensional NMR data. The rate of formation of disaccharide pNP-1,4-GlcXyl (Figure 1, compound 8) was found to be 3.3 times that of pNP-1,3-GlcXyl (Figure 1, compound 7), another surprising result in light of  $\beta$ -1,3-linkages being preferred ahead of  $\beta$ -1,4-linkages when pNPGlc was used as the acceptor. It is also apparent that newly formed pNP-1,4-GlcXyl becomes a favored acceptor for the synthesis of the pNP-1,6-1,4-GlcGlcXyl trisaccharide (Figure 1, compound 9). After 72 h, there is a decline in the level of formation of the three main products as larger products ( $n = 4, 5$ , or  $6$ ) were forming (as shown by TLC and MS), but because of the very small amounts involved, these could not be characterized in terms of their specific linkages.

**Crystal Structures.** A structural explanation for the unexpected regioselectivity of the glycosynthase reaction was sought by sequentially soaking donor and acceptor species into a crystal of E292S Exg with the knowledge that catalytic turnover would not be an issue for the relatively short time scale involved prior to crystal freezing. The structures of both the variant alone and its ternary complex were determined to 1.9 Å resolution (Table 1). The ternary complex structure is the first to show both donor and acceptor species, i.e., the two substrates, bound together in a glycosynthase (Figure 4A).

The donor  $\alpha$ -GlcF was found to occupy the  $-1$  subsite as expected, in a <sup>4</sup>C<sub>1</sub> chair conformation with the fluorine atom directed at the hydroxyl of Ser 292 but not quite within hydrogen bonding distance (Figure 4C). Instead, it interacts with a bridging water molecule that hydrogen bonds to the serine hydroxyl and whose position corresponds to a carboxylate oxygen of E292 in the native structure. A time course tracked by TLC (Figure 2A, right panel) showed that hydrolysis of  $\alpha$ -GlcF to D-glucose was much slower than the crystal soak time with the two substrates; hence, it may be assumed that the crystal structure contains both active donor and acceptor species. The acceptor molecule pNPGlc was seen lying between the two almost parallel side chains of F144 and F258 that largely define the  $+1$  subsite and is stabilized mainly by CH– $\pi$  interactions, with only one direct hydrogen bond to the protein, viz., sugar C4-OH group to the N146 side chain. The nearest hydroxyl to the anomeric carbon of  $\alpha$ -GlcF is on C6, and although there is some disorder associated with this hydroxyl group (as seen in its low occupancy), it is reasonably positioned for backside attack on the anomeric carbon. Free

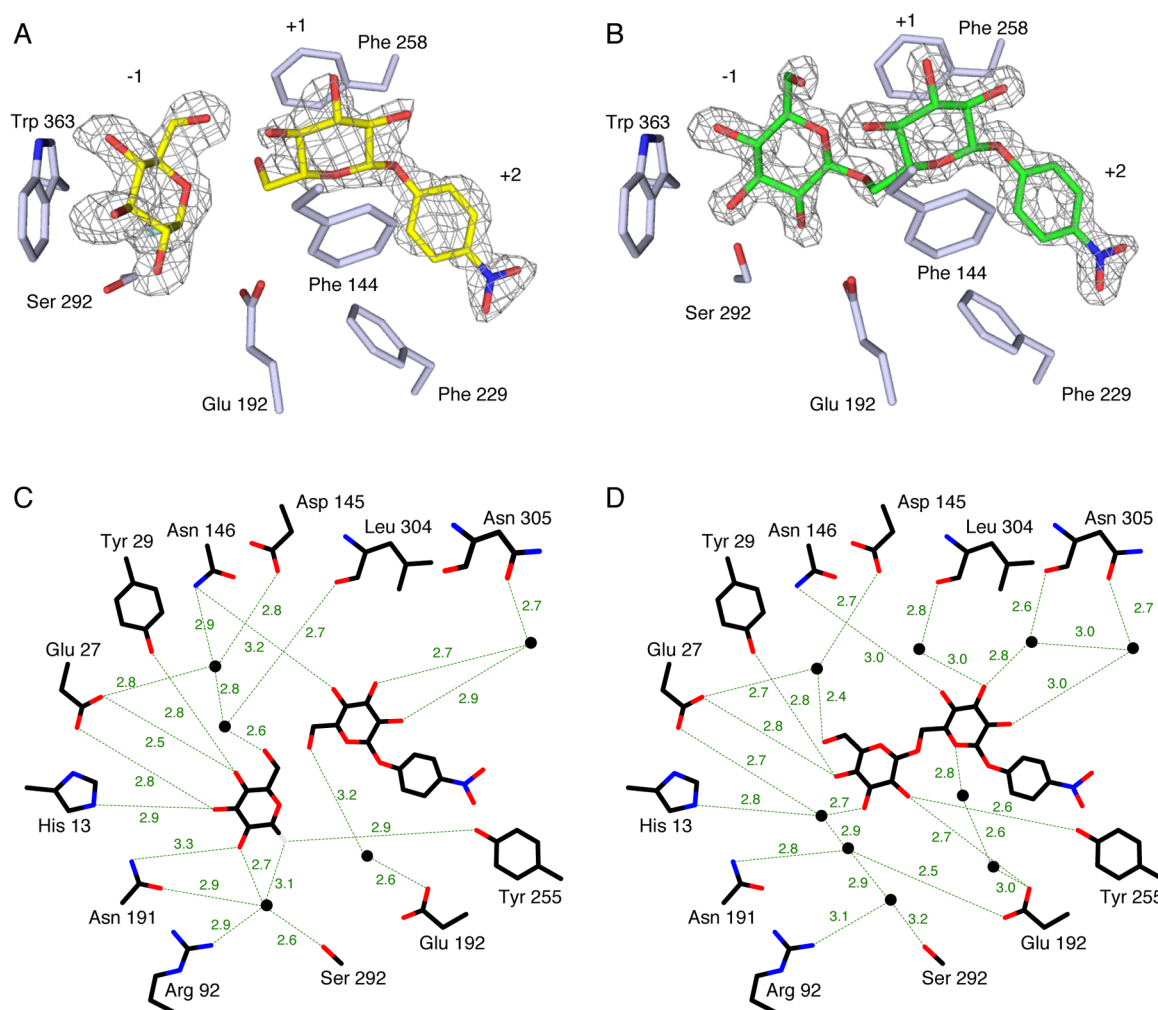


**Figure 4.** Binding of donor  $\alpha$ -GlcF and acceptor pNPGlc, and of product pNP-gentiobiose, to E292S Exg. (A and B)  $F_o - F_c$  omit maps contoured at  $2.5\sigma$  and  $3.0\sigma$ , respectively, showing electron density in the active site region. (C and D) LIGPLOT figures showing hydrogen bonds involving sugars, protein, and water molecules. The carbohydrate binding subsites on the enzyme are labeled -1, +1, and +2, with catalysis occurring between subsites -1 and +1, as per the nomenclature adopted for glycosyl hydrolases.<sup>38</sup>

rotation about the C5–C6 bond would allow a better angle of attack for the  $S_N2$ -like reaction mechanism. It is evident then that the preferred orientation of the acceptor species favors  $\beta$ -1,6-linkage formation both in the crystal and in solution. The *p*-nitrophenyl group interacts with the protein in a  $\pi$  stacking arrangement<sup>30</sup> at a center-normal angle of  $40^\circ$  to, and  $\sim 4.8$  Å from (ring centroid to centroid), the phenylalanine ring of F229, the putative +2 subsite.<sup>19</sup>

To examine how the glycosynthase variant binds to the major product, pNP-gentiobiose, the structure of this complex was determined to 1.6 Å resolution (Table 1). The major finding was that the pNPGlc moiety was oriented exactly as seen with the acceptor pNPGlc in the two-substrate structure; however, the first glucose residue was partially displaced from the -1 subsite, allowing two water molecules in to replace the C2-OH and C3-OH groups of the donor molecule  $\alpha$ -GlcF (Figure 4B,D). The position of the C4 hydroxyl group of the terminal sugar is the same in the two structures (Figure 5A), held by hydrogen bonds to E27 and Y29, and acting as a pivot about which the sugar ring has rotated. The LIGPLOT comparison (Figure 4C,D) shows the hydrogen bonding networks in the two structures and in particular the role played by the two bridging waters in the -1 site. Interestingly, the structure of the

E292S variant alone shows seven well-resolved water molecules in the -1 site that are imprints of the C2, C3, C4 (common), and C6 sugar hydroxyls of  $\alpha$ -GlcF and the pNP-gentiobiose nonreducing end (see Figure S3 of the Supporting Information). Moreover, the native Exg structure (PDB entry 1CZ1) has the same disposition of seven waters showing that the mutation of the catalytic nucleophile E292 to a serine does not affect this telltale arrangement of water molecules. Overall, then, it appears as if the -1 site of Exg has evolved to accommodate the terminal glucose moiety in either of two positions.

## DISCUSSION

For retaining glycosidases, their glycosynthase potential has been predicted by examination of kinetic parameters for the turnover of the glycosyl-enzyme intermediate.<sup>31</sup> For a glycosidase to become an active glycosynthase, it needs to show high selectivity for transfer to the acceptor over water. Using reactivation parameters derived for Exg,<sup>32</sup> it was predicted that Exg would make a relatively poor glycosynthase using an aryl  $\beta$ -glucoside acceptor. This proved to be the case as seen in the results presented here for E292S Exg. However, this low-level glycosynthase activity permitted direct (crystallo-



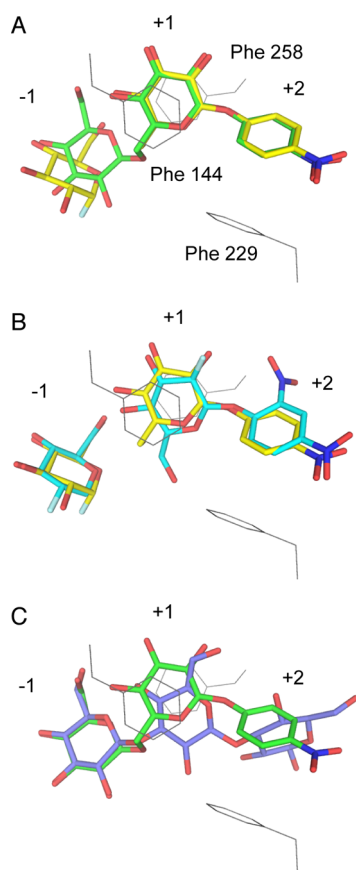


**Figure 5.** Comparisons of the binding positions and orientations of various carbohydrate species complexed to  $\beta$ -1,3-exoglucanase variants of *C. albicans*. Binding sites  $-1$  and  $+1$  have been superimposed. (A) Overlap of donor  $\alpha$ -GlcF and acceptor pNPGlc (yellow) with product pNP-gentiobiose (green), as seen in complex with E292S Exg. (B) Overlap of  $\alpha$ -GlcF with pNPGlc (yellow) and inhibitor DNP2FGlc (cyan) bound to native Exg. (C) Superposition of pNP-gentiobiose (green) and laminaritrise (purple) as bound to F229A/E292S Exg.

graphic) observation of an enzyme complex involving both donor and acceptor species and with it provided some valuable insights into the enzyme's regiospecificity and overall mode of action. This is the first structural description of a glycosynthase in complex with both of its substrates; indeed, there is only one other structure in the Protein Data Bank of a glycosynthase shown complexed to the commonly used donor substrate  $\alpha$ -GlcF,<sup>33</sup> another containing  $\alpha$ -laminariheptaosyl fluoride,<sup>34</sup> and a total of just seven glycosynthase structures in all.

The solution studies with E292S Exg have revealed the formation of three different glucosidic linkages in the predominantly disaccharide products, with  $\beta$ -1,6-linkages strongly favored over  $\beta$ -1,3- and  $\beta$ -1,4-linkages. This surprising result caused us to ask why this glycosynthase prefers to form  $\beta$ -1,6-linkages when WT Exg strongly favors  $\beta$ -1,3-linkages for both hydrolysis and glucosyl transfer and, specifically, whether this might be due to the influence of the pNP moiety of the acceptor species in directing the orientation of the sugar at the  $+1$  site.

The crystallographic results presented here support this conclusion as the nitrophenyl groups of both the acceptor pNPGlc and product (pNP-gentiobiose) stack against F229 rather than pointing away from the surface of the enzyme. Further support comes from an earlier observation, puzzling at

the time,<sup>18</sup> that an unreacted molecule of the mechanism-based inactivator, dinitrophenyl 2-deoxy-2-fluoro- $\beta$ -D-glucopyranoside (DNP2FGlc), bound to native Exg at the  $+1$  and  $+2$  subsites in a very similar manner (Figure 5B); i.e., it was positioned for  $\beta$ -1,6-activity and not  $\beta$ -1,3-activity. The aqueous solution results obtained from this study indicate a flexibility in sugar positioning and orientation between the side chains of F258 and F144 at the  $+1$  site, a property that is needed to explain the different linkages observed with the glycosynthesis reactions. This conclusion is supported by a recent crystallographic study of laminaritrise (a trisaccharide of three  $\beta$ -1,3-linked D-glucopyranose units) bound to the F229A/E292S variant of Exg<sup>19</sup> in which the second sugar is not only held in a different position by the Phe-Phe clamp (the  $+1$  site) but also flipped 180° and displaced relative to that seen in the gentiobiose structure (Figure 5C and Figure S4 of the Supporting Information). This positions the C3 hydroxy group for interaction with C1 of the terminal sugar at the  $-1$  site and allows the two-bond 1,3-glycosidic linkage to be made, as opposed to the three-bond 1,6-linkage. For 1,4-linkage to occur, a small swivel of the sugar in the aromatic clamp is required rather than an inversion. The finding that the biose pNP-1,4-GlcXyl was also an acceptor for  $\beta$ -1,6-directed glycosynthesis was interesting as the nitrophenyl group would now be located beyond F229, but without crystal structure evidence to show how this molecule interacts with the enzyme, no conclusion can be drawn.

These studies demonstrate an unexpected flexibility in sugar binding at the  $+1$  site of Exg as previously it had been suggested that the Phe-Phe clamp would restrict Exg specificity to  $\beta$ -1,3 linkages compared to the broader Trp-Trp clamp seen in some other exoglucanases, notably the barley  $\beta$ -D-glucan glucosylhydrolase (a GH3 family member), which allows hydrolysis of  $\beta$ -1,2-,  $\beta$ -1,3-,  $\beta$ -1,4-, and  $\beta$ -1,6-linkages.<sup>35</sup> The versatility of the Phe-Phe clamp is presumably important for the activity of Exg in the *Candida* cell wall where branched  $\beta$ -D-glucan is a major component. Evidence to date has shown  $\beta$ -1,3-specificity of Exg is significantly stronger than  $\beta$ -1,6-specificity, but these assays have mainly involved short linear oligosaccharides as well as laminarin, a seaweed-derived, moderate-sized polymer of  $\beta$ -1,3-D-glucan sometimes containing several  $\beta$ -1,6-branch points. It might be argued then that these substrates may not properly represent the meshed cell wall glucan structure and that a nonlinear substrate might be presented in such a manner to allow  $\beta$ -1,6-glucosidase/transglycosidase activity. The identification of a secondary carbohydrate binding site well removed from the active site<sup>19</sup> indirectly supports this proposal as it suggests several points of binding. With regard to the unexpected  $\beta$ -1,4-activity, it is worth noting that Exg is a member of the very large and diverse GH5 family,<sup>36</sup> many of whose members are  $\beta$ -1,4-endoglucanases (cellulases) while others show  $\beta$ -1,6-activity; thus, this family has evolved from a ( $\beta/\alpha$ )<sub>8</sub> scaffold to be versatile with respect to sugar binding orientations.

Finally, the observation that the  $-1$  site can hold the terminal sugar in one of two positions would suggest that one position is aligned for catalysis whereas the other lies on the pathway for substrate docking or product release. We are unaware of any other such active site arrangement in a glycoside hydrolase. This hypothesis is supported by the presence of well-defined water molecules seen in both the glycosynthase and native Exg structures, which correspond to both sets of sugar hydroxyl positions.



It is worth noting that there are relatively few glycosynthase reactions reported in the literature that show  $\beta$ -1,6-regiospecificity.<sup>7</sup> The first landmark example involved the E537S mutant of *Escherichia coli*  $\beta$ -galactosidase, which catalyzed the formation of a  $\beta$ -1,6-linked disaccharide product from  $\alpha$ -GalF and pNPGlc. This was in contrast to the  $\beta$ -1,4-regiochemistry displayed in the WT hydrolysis reaction, but consistent with its  $\beta$ -1,6 transglycosylation specificity.<sup>37</sup> Such behavior is quite different from that shown by Exg in the study presented here.

In conclusion, this study has provided firm evidence that (a) an aryl substituent on the acceptor molecule can indeed influence regiospecificity in glycosynthase reactions, (b) the *Candida* cell wall exoglucanase might exhibit specificity broader than previously thought, and (c) ordered water molecules in the active site of a glycosynthase, or its parent enzyme, accurately plot the path of sugar binding. In more general terms, it reinforces the relevance of protein–ligand crystal structures to favored reactions in solution and provides an example of an enzyme complexed to both of its reactants in crystal.

## ■ ASSOCIATED CONTENT

### ■ Supporting Information

TLC analysis of pNP derivatives for E292S and E292G Exg glycosynthases using pNPGlc as the acceptor (Figure S1), TLC and HPLC analyses of E292S Exg using pNPXyl as the acceptor (Figure S2), structural representations of water molecules in the active site of E292S Exg (Figure S3), comparison of bound pNP-gentiobiose and laminaritrise in the binding cleft (Figure S4), and one- and two-dimensional NMR spectral data for both glycosynthase reactions. This material is available free of charge via the Internet at <http://pubs.acs.org>.

## ■ AUTHOR INFORMATION

### Corresponding Author

\*E-mail: [john.cutfield@otago.ac.nz](mailto:john.cutfield@otago.ac.nz). Phone: +64 3 479 7841.

### Notes

The authors declare no competing financial interest.

## ■ ACKNOWLEDGMENTS

We thank Dr. James Macdonald and Professor Steven Withers of the University of British Columbia for providing  $\alpha$ -D-glucopyranosyl fluoride and for performing a preliminary glycosynthesis experiment with our E292S Exg variant that indicated a mixture of products was formed. Bronwyn Carlisle assisted with the production of figures.

## ■ ABBREVIATIONS

Exg,  $\alpha$ -1,3- $\beta$ -glucanase from *C. albicans*;  $\alpha$ -GlcF,  $\alpha$ -D-glucopyranosyl fluoride; pNPGlc, *p*-nitrophenyl  $\beta$ -D-glucopyranoside; pNPXyl, *p*-nitrophenyl  $\beta$ -D-xylopyranoside; CAZY, carbohydrate-active enzyme; GH, glycoside hydrolase; *p*-nitrophenyl  $\beta$ -D-gentiobiose, *p*-nitrophenyl 6-O-( $\beta$ -D-glucopyranosyl)- $\beta$ -D-glucopyranoside; pNP, *p*-nitrophenyl; HPLC, high-performance liquid chromatography; NMR, nuclear magnetic resonance; LCQ, liquid chromatography quadrupole; ESI, electrospray ionization; WT, wild type; TLC, thin layer chromatography; gHMBC, gradient-selected heteronuclear multiple-bond correlation; NOESY, nuclear Overhauser effect spectroscopy; HSQC, heteronuclear single-quantum coherence; COSY, correlation spectroscopy; pNP-laminaribioside, *p*-

nitrophenyl 3-O-( $\beta$ -D-glucopyranosyl)- $\beta$ -D-glucopyranoside; pNP-cellobioside, *p*-nitrophenyl 4-O-( $\beta$ -D-glucopyranosyl)- $\beta$ -D-glucopyranoside; pNP-1,4-GlcXyl, *p*-nitrophenyl 4-O-( $\beta$ -D-glucopyranosyl)- $\beta$ -D-xylopyranoside; pNP-1,3-GlcXyl, *p*-nitrophenyl 3-O-( $\beta$ -D-glucopyranosyl)- $\beta$ -D-xylopyranoside; pNP-1,6-1,4-GlcGlcXyl, *p*-nitrophenyl 6-O-( $\beta$ -D-glucopyranosyl)-4-O-( $\beta$ -D-glucopyranosyl)- $\beta$ -D-xylopyranoside; MS, mass spectrometry; DNP2FGlc, dinitrophenyl-2-deoxy-2-fluoro- $\beta$ -D-glucopyranoside; PDB, Protein Data Bank.

## ■ REFERENCES

- (1) McKenzie, L. F.; Wang, Q.; Warren, R. A. J., and Withers, S. G. (1998) Glycosynthases: Mutant glycosidases for oligosaccharide synthesis. *J. Am. Chem. Soc.* 120, 5583–5584.
- (2) Malet, C., and Planas, A. (1998) From  $\beta$ -glucanase to  $\beta$ -glucansynthase: Glycosyl transfer to  $\alpha$ -glycosyl fluorides catalysed by a mutant endoglucanase lacking its catalytic nucleophile. *FEBS Lett.* 440, 208–212.
- (3) Fort, S., Boyer, V., Greffe, L., Davies, G. J., Moroz, O., Christiansen, L., Schulein, L., Cottaz, S., and Driguez, H. (2000) Highly efficient synthesis of  $\beta$ -(1,4)-oligo- and -polysaccharides using a mutant cellulase. *J. Am. Chem. Soc.* 122, 5429–5437.
- (4) Fajies, M., Imai, T., Bulone, V., and Planas, A. (2004) In vitro synthesis of a crystalline (1 $\rightarrow$ 3,1 $\rightarrow$ 4)- $\beta$ -D-glucan by a mutated (1 $\rightarrow$ 3,1 $\rightarrow$ 4)- $\beta$ -D-glucanase from *Bacillus*. *Biochem. J.* 380, 635–641.
- (5) Perugini, G., Trincone, A., Rossi, M., and Moracci, M. (2004) Oligosaccharide synthesis by glycosynthases. *Trends Biotechnol.* 22, 31–37.
- (6) Fajies, M., and Planas, A. (2007) In vitro synthesis of artificial polysaccharides by glycosidases and glycosynthases. *Carbohydr. Res.* 342, 1581–1594.
- (7) Hancock, S. M., Vaughan, M. D., and Withers, S. G. (2006) Engineering of glycosidases and glycosyltransferases. *Curr. Opin. Chem. Biol.* 10, 509–519.
- (8) Shaikh, F. A., and Withers, S. G. (2008) Teaching old enzymes new tricks: Engineering and evolution of glycosidases and glycosyl transferases for improved glycoside synthesis. *Biochem. Cell Biol.* 86, 169–177.
- (9) Hommalai, G., Withers, S. G., Chuenchor, W., Cairns, J. R. K., and Svasti, J. (2007) Enzymatic synthesis of cello-oligosaccharides by rice BGlu1  $\beta$ -glucosidase glycosynthase mutants. *Glycobiology* 17, 744–753.
- (10) Fajies, M., Saura-Valls, M., Perez, X., Conti, M., and Planas, A. (2006) Acceptor-dependent regioselectivity of glycosynthase reactions by *Streptomyces* E383A  $\beta$ -glucosidase. *Carbohydr. Res.* 341, 2055–2065.
- (11) Stick, R. V., Stubbs, K. A., and Watts, A. G. (2004) Modifying the regioselectivity of glycosynthase reactions through changes in the acceptor. *Aust. J. Chem.* 57, 779–786.
- (12) Cantarel, B. L., Coutinho, P. M., Rancurel, C., Bernard, T., Lombard, V., and Henrissat, B. (2009) The Carbohydrate-Active EnZymes database (CAZY): An Expert Resource for Glycogenomics. *Nucleic Acids Res.* 37, D233–D238.
- (13) Martin, K., McDougall, B. M., McIlroy, S., Chen, J., and Seviour, R. J. (2007) Biochemistry and molecular biology of exocellular fungal  $\beta$ -(1,3)- and  $\beta$ -(1,6)-glucanases. *FEMS Microbiol. Rev.* 31, 168–192.
- (14) Chaffin, W. L. (2008) *Candida albicans* cell wall proteins. *Microbiol. Mol. Biol. Rev.* 72, 495–544.
- (15) De Groot, P. W. J., Brandt, B. W., and Klis, F. M. (2007) Cell Wall Biology of *Candida*. In *Candida Comparative and Functional Genomics* (d'Enfert, C., and Hube, B., Eds.) pp 294–325, Caister Academic Press, Norfolk, U.K.
- (16) Iorio, E., Torasantucci, A., Bromuro, C., Chiani, P., Ferretti, A., Giannini, M., Cassone, A., and Podo, F. (2008) *Candida albicans* cell wall comprises a branched  $\beta$ -D-(1 $\rightarrow$ 6)-glucan with  $\beta$ -D-(1 $\rightarrow$ 3)-side chains. *Carbohydr. Res.* 343, 1050–1061.
- (17) Stubbs, H. J., Brasch, D. J., Emerson, G. W., and Sullivan, P. A. (1999) Hydrolase and transferase activities of the  $\beta$ -1,3-exoglucanase of *Candida albicans*. *Eur. J. Biochem.* 263, 889–895.

- (18) Cutfield, S. M., Davies, G. J., Murshudov, G., Anderson, B. F., Moody, P. C., Sullivan, P. A., and Cutfield, J. F. (1999) The structure of the exo- $\beta$ -(1,3)-glucanase from *Candida albicans* in native and bound forms: Relationship between a pocket and groove in family 5 glycosyl hydrolases. *J. Mol. Biol.* 294, 771–783.
- (19) Patrick, W. M., Nakatani, Y., Cutfield, S. M., Sharpe, M. L., Ramsay, R. J., and Cutfield, J. F. (2010) Carbohydrate binding sites in *Candida albicans* exo- $\beta$ -(1,3)-glucanase and the role of the Phe-Phe 'clamp' at the active site entrance. *FEBS J.* 277, 4549–4561.
- (20) Horton, R. M., Cai, Z. L., Ho, S. N., and Pease, L. R. (1990) Gene splicing by overlap extension: Tailor-made genes using the polymerase chain reaction. *BioTechniques* 8, 528–535.
- (21) Winn, M. D., et al. (2011) Overview of the CCP4 suite and current development. *Acta Crystallogr. D* 67, 235–242.
- (22) McCoy, A. J., Grosse-Kunstleve, R. W., Adams, P. D., Winn, M. D., Storoni, L. C., and Read, R. J. (2007) Phaser crystallographic software. *J. Appl. Crystallogr.* 40, 658–674.
- (23) Emsley, P., Lohkamp, B., Scott, W. G., and Cowtan, K. (2010) Features and development of Coot. *Acta Crystallogr. D* 66, 486–501.
- (24) Adams, P. D., Afonine, P. V., Bunkóczy, G., Chen, V. B., Davis, I. W., Echols, N., Headd, J. J., Hung, L.-W., Kapral, G. J., Grosse-Kunstleve, R. W., McCoy, A. J., Moriarty, N. W., Oeffner, R., Read, R. J., Richardson, D. C., Richardson, J. S., Terwilliger, T. C., and Zwart, P. H. (2010) PHENIX: A comprehensive Python-based system for macromolecular structure solution. *Acta Crystallogr. D* 66, 213–221.
- (25) Vaguine, A. A., Richelle, J., and Wodak, S. J. (1999) SFCHECK: A unified set of procedures for evaluating the quality of macromolecular structure factors and their agreement with the atomic model. *Acta Crystallogr. D* 55, 191–305.
- (26) Wallace, A. C., Laskowski, R. A., and Thornton, J. M. (1996) LIGPLOT: A program to generate schematic diagrams of protein-ligand interactions. *Protein Eng.* 8, 127–134.
- (27) Freimund, S., Huwig, A., Giffhorn, F., and Kopper, S. (1998) Rare keto-aldehydes from enzymatic oxidation: Substrates and oxidation products of pyranose-2-oxidase. *Chem. Eur. J.* 4, 2442–2454.
- (28) Nozaki, K., Kano, A., Amano, Y., Murata, T., Usui, T., Ito, K., and Kanda, T. (2004) Transglycosylation reaction and acceptor specificity of exo- and endo-type cellulases. *J. Appl. Glycosci.* 51, 87–92.
- (29) Wei, J., Lv, X., Lu, Y., Yang, G., Fu, L., Yang, L., Wang, J., Gao, J., Cheng, S., Duan, Q., Jin, C., and Li, X. (2013) Glycosynthase with broad substrate specificity: An efficient biocatalyst for the construction of oligosaccharide library. *Eur. J. Org. Chem.* 2013, 2414–2419.
- (30) McGaughey, G. B., Gagne, M., and Rappe, A. K. (1998)  $\pi$ -stacking interactions: Alive and well in proteins. *J. Biol. Chem.* 273, 15458–15463.
- (31) Ducros, V. M.-A., Tarling, C. A., Zechel, D. L., Brzozowski, A. M., Frandsen, T. P., von Ossowski, I., Schuelein, M., Withers, S. G., and Davies, G. J. (2003) Anatomy of glycosynthesis: Structure and kinetics of the *Humicola insolens* Cel7B E197A and E197S glycosynthase mutants. *Chem. Biol.* 10, 619–628.
- (32) Mackenzie, L. F., Brooke, G. S., Cutfield, J. F., Sullivan, P. A., and Withers, S. G. (1997) Identification of Glu-330 as the catalytic nucleophile of *Candida albicans* exo- $\beta$ -(1,3)-glucanase. *J. Biol. Chem.* 272, 3161–3167.
- (33) Pengthaisong, S., Withers, S. G., Kuaprasert, B., Svasti, J., and Cairns, J. R. K. (2012) The role of the oligosaccharide binding cleft of rice BGlu1 in hydrolysis of cellooligosaccharides and in their synthesis by rice BGlu1 glycosynthase. *Protein Sci.* 21, 362–372.
- (34) Vasur, J., Kawai, R., Jonsson, K. H. M., Widmalm, G., Engstrom, A., Frank, M., Andersson, E., Hansson, H., Forsberg, Z., Igarashi, K., Samejima, M., Sandgren, M., and Stahlberg, J. (2010) Synthesis of cyclic  $\beta$ -glucan using laminarinase 16A glycosynthase mutant from the basidiomycete *Phanerochaete chrysosporium*. *J. Am. Chem. Soc.* 132, 1724–1730.
- (35) Hrmova, M., and Fincher, G. B. (2007) Dissecting the catalytic mechanism of a plant  $\beta$ -D-glucan glucosylhydrolase through structural biology using inhibitors and substrate analogues. *Carbohydr. Res.* 342, 1613–1623.
- (36) Aspeborg, H., Coutinho, P. M., Wang, Y., Brumer, H., III, and Henrissat, B. (2012) Evolution, substrate specificity and subfamily classification of glycoside hydrolase family 5 (GH5). *BMC Evol. Biol.* 12, 186.
- (37) Jakeman, D. L., and Withers, S. G. (2002) On expanding the repertoire of glycosynthases: Mutant  $\beta$ -galactosidases forming  $\beta$ -(1,6)-linkages. *Can. J. Chem.* 80, 866–870.
- (38) Davies, G. J., Wilson, K. S., and Henrissat, B. (1997) Nomenclature for sugar-binding subsites in glycosyl hydrolases. *Biochem. J.* 221, 557–559.